# Formation of laser plasma channels in a stationary gas

A. Dunaevsky
*Department of Astrophysical Sciences, Princeton University, Princeton, New Jersey 08540*

A. Goltsov
*Troitsk Institute of Innovative and Thermonuclear Research (TRINITI), Troitsk 142190, Russia*

J. Greenberg
*School of Engineering and Applied Science, Department of MAE, Princeton University, Princeton, New Jersey 08544*

E. Valeo and N. J. Fisch
*Princeton Plasma Physics Laboratory, P.O. Box 451, Princeton, New Jersey 08543*

(Received 18 November 2005; accepted 21 March 2006; published online 27 April 2006)

Plasma channels with nonuniformity of about ±3.5% have been produced by a 0.3 J, 100 ps laser pulses in a nonflowing gas, contained in a cylindrical chamber. The laser beam passed through the chamber along its axis via pinholes in the chamber walls. Plasma channels with an electron density in the range of $10^{18}-10^{19}$ $cm^{-3}$ were formed in pure He, $N_2$, Ar, and Xe. A uniform channel forms in an optimal pressure range at a certain time delay, depending on the gas molecular weight. The interaction of the laser beam with the gas leaking out of the chamber through the pinholes was not significant. However, the formation of the ablative plasma on the walls of pinholes by the wings of radial profile of the laser beam plays an important role in the plasma channel formation and its uniformity. A low-current glow discharge initiated in the chamber improves the uniformity of the plasma channel slightly, while a high-current arc discharge leads to overdense plasma near the front pinhole and further refraction of the laser beam. These results indicate the potential for using nonflowing gas targets to create uniform plasma channels. © *2006 American Institute of Physics*. [DOI: 10.1063/1.2195383]

## I. INTRODUCTION

With chirped pulse amplification technique (CPA), power densities of the order of $10^{20}$ $W/cm^2$ in focused beam are available only with meter-size gratings. Recently, several schemes of stimulated Raman backscattering (SRB) in plasma have been proposed to overcome material limitations of CPA and thereby allow power densities several orders of magnitude higher with moderate-scale systems.[1–4] While there is the possibility of efficient SRB using an ionizing laser beam on the ionization front of an initially neutral gas,[3] the majority of the approaches rely on the interaction between counterpropagating pump and seed beams in a precreated plasma channel. The amplification regimes for the precreated plasma have been worked out.[4] The key aspects of resonant Raman backscattering scheme enjoy significant laboratory verification.[5]

However, being essentially a resonant three-wave process, the SRB amplification is sensitive to the plasma frequency $\omega_p$. The resonance can be detuned by longitudinal fluctuations of the electron density $\delta n_{ez}$, which give rise to electron plasma wave frequency fluctuations $\delta\omega_p = \omega_p \delta n_{ez}/2n_{e0}$. Here, $\omega_p=(4\pi e^2 n_{e0}/m_e)^{1/2}$ is the plasma frequency and $n_{e0}$ is the electron density in the plasma channel. For efficient amplification, the frequency fluctuations should be less than the bandwidth of the pumping beam, which is about twice the SRB linear growth rate $\Delta\omega \sim 2\gamma = a_0(\omega\omega_p)^{1/2}$.[6] Thus, for linear amplification, the maximal allowable fluctuation of the plasma density is

$$\frac{\delta n_{ez}}{n_e} < a_0 \sqrt{\frac{\omega}{\omega_p}}, \tag{1}$$

where $a_0=eE/mc\omega$ is normalized electric field in the beam. In practice, in the linear amplification regime, the nonuniformity generally ought to be less than a few percent.

For nonlinear amplification, the limitation on allowable density fluctuations is modified. Solodov *et al.*[6] showed that for a given length $L$ of a uniform plasma channel the average fluctuation amplitude should be less than

$$\frac{\delta n_{ez}}{n_e} < \frac{2\omega c}{\omega_p^2 \sqrt{L l_\parallel}}, \tag{2}$$

where $l_\parallel$ is a longitudinal correlation length. For experimental beam parameters and $l_\parallel \approx 0.2$ mm, the density nonuniformity has to be $\delta n_{ez}/n_e < 3-4\%$.

In the first experimental arrangements, plasma with a density of $n_e \sim 10^{20}$ $cm^{-3}$ and a temperature of $T_e \sim 20$ eV was created in a capillary by KrF laser.[7,8] It was shown, however, that the effective length of the plasma channel in copper and LiF capillaries did not exceed 0.2 mm, presumably due to intense pump absorption via inverse bremsstrahlung mechanism and initial nonuniformity of the plasma density in the capillary. At lower plasma densities, amplification with $K=\exp(2\gamma L/c) \sim 100$ has been demonstrated recently with Ar-filled glass capillary.[9] However, the experimentally achieved amplification was lower by several orders of mag-

 

nitude than what would be predicted theoretically for a completely uniform channel.

Alternatively, high-density gas jets ionized by Nd:YAG laser can provide reproducible plasma channels of 1–2 mm length with a density of $n_e \sim 10^{19}$ cm$^{-3}$ and a temperature of $T_e \sim 5$ eV. At this order of plasma density, pump absorption due to inverse bremsstrahlung becomes less important, and amplification ratios up to $K \sim 10^3$ were obtained.[5,10] The possibility to measure the density profile directly in the jet plasma is an additional advantage of the method. However, turbulence in the flow from a nozzle affects the uniformity of the neutral gas density in the flow and, consequently, leads to significant plasma density nonuniformity. At present, the short effective length $L$ is probably the main practical limitation of the SRB amplification.[5]

The motivation for the present work is an alternative technology to gas jets for coupling the counterpropagating laser beams in high-power pulse compression by resonant Raman backscattering. Nonflowing gas might overcome the difficulties in creation of uniform plasma channel in flowing gas. The creation of tubular plasma channels in stationary, nonflowing gas was first proposed by Durfee and Milchberg for guiding high-intensity laser beams.[11] In a backfill gas at pressures of about 30–200 Torr, plasma channels with an electron density of $1-4\times10^{18}$ cm$^{-3}$ and a length of $\sim$1.2 mm were formed by Nd:YAG laser beam with a power density of $\sim 4\times10^{14}$ W/cm$^2$, focused by an aplanatic lens. Longer channels were created with the use of an axicon for linear focusing of the ionizing laser beam. Through shock expansion, the channel forms a tubular plasma waveguide, which is effective for guiding high-intensity laser beams over several Rayleigh lengths.[12] These plasma channels were studied experimentally and numerically.[13,14] Gaul *et al.*[15] reported the creation of a 1.5 cm long channel in 400 Torr He backfill by axicon-focused Nd:YAG beam, using either long ($\sim$400 ps) 0.6 J pulses or 100 ps, 0.3 J pulses together with a pulsed arc discharge for preionization.

While the ionization of stationary gas in a backfill chamber is a promising technique for creation of elongated uniform plasma channels, it is not applicable directly for SRB amplification. High-power pump and seed beams, as well as the ultrahigh power amplified beam, cannot be transported to the plasma channel in dense neutral gas without intense interaction with the gas. For such applications, the gas should be localized in a container placed in an evacuated chamber. The container should have windows to let the interacting and ionizing beams penetrate the gas volume.

With the application of SRB in mind, we demonstrate in this paper the possibility to create plasma channels several millimeters long, with relatively high uniformity and relatively high electron density, in a cylindrical gas container having pinholes to let powerful laser beams enter the plasma channel directly.

## II. EXPERIMENTAL SETUP

Figure 1 presents a sketch of the experimental setup. The gas target can be represented as a cylinder with a diameter of 10 mm and a length of 3 mm. The cylinder has two pinholes,

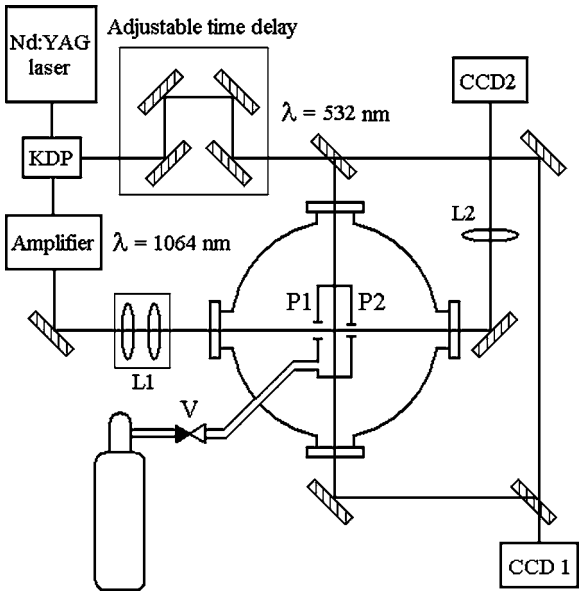


FIG. 1. Experimental setup.

$P1$ and $P2$ (see Fig. 1), on its end walls to let the laser beams go throughout the cylinder. The pinholes are made of copper and aligned with the cylinder axis. The optimal diameter of the pinholes is determined by the balance between the minimal possible gas leak out of the cylinder and minimal losses of the ionizing beam due to pinhole closure. The gas is supplied into the cylinder through a needle valve $V$. The feeding gas pipe has a distributor made of porous metal to decrease possible density nonuniformities induced by incoming gas flow. The gas pressure in the cylinder is monitored by a miniature pressure transducer. The optical access to the plasma is provided trough a pair of optically flat windows made in the sidewalls of the cylinder. The cylinder is installed in a vacuum chamber with a diameter of about 35 cm on a 5-degrees-of-freedom kinematic stage. The background pressure in the chamber was kept at 300–600 mTorr by a mechanical pump.

An ionizing beam of Nd:YAG laser ($\lambda = 1064$ nm) had an energy in the range 0.1–0.7 J and a duration of $\tau_b = 100$ ps. An initially rectangular beam of $5\times1$ cm at the output of a slab amplifier was focused onto the gas target by a pair of cylindrical lenses $L1$. The beam size at the waist point was $\sim 70\times70$ $\mu$m full width at half magnitude (FWHM). Shape of the beam and its alignment with the pinholes was monitored by a TV camera CCD2 though a telescope $L2$.

Series of special experiments showed the absence of significant interaction of laser beam with the gas flowing out the cylinder through the pinholes.

The plasma density distribution in the channel was measured by a Mach-Zehnder interferometer set up on the second harmonics ($\lambda = 532$ nm) probe beam, which was split out of the ionizing beam. Interferograms were registered by a camera CCD1. The radial spread of the plasma was observed by adding a time delay into the probe beam. The phase shift profiles retrieved from interferograms were then processed to

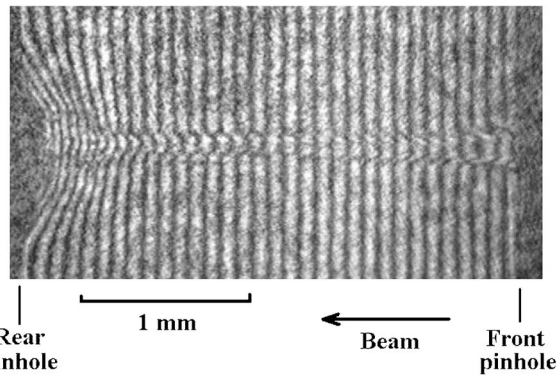


FIG. 2. Typical interferograms of the plasma channel. Arrow shows the beam direction. $J_{in}=0.38$ J, $p=90$ Torr $N_2$.

restore the radial density distribution by an inverse Abel transform algorithm.[16]

## III. EXPERIMENTAL RESULTS AND DISCUSSION

### A. General appearance

A typical interferogram of the plasma channel, taken at a delay of $\tau=800$ ps from the beginning of the ionizing beam, is presented in Fig. 2. Channels with similar structures were observed in nitrogen in the pressure range of 20–300 Torr, in He at pressures higher than ~200 Torr, and in Xe at 30–80 Torr. Channels are formed by laser beams with energy from ~0.2 J and higher. The initial plasma spark is formed mainly due to tunneling ionization,[17] like for the backfill and gas jets. Plasma electrons are heated in the laser field due to collisional absorption of laser energy, and drive further ionization by ion-electron collisions. Highly nonequilibrium plasma expands into the neutral gas, forming a shock wave and minimum of plasma density at the axis.[9] Density of the plasma channels decays fast; no indication of plasma with density above $10^{18}$ $cm^3$ was observed on the interferograms after 2.5 ns from the laser pulse.

While the scenario of the channel formation is similar to backfill and gas jets, several distinctive features are apparent. First, at the entrance (right side on the interferogram), the plasma channels are always wider and shrink gradually along the channel. Such a gradual decrease downstream of the front pinhole was observed in all experiments with the beam waist at the middle of the gas cylinder. Positioning of the beam waist at the plane of the rear pinhole leads to high nonuniformity of the channel profile, with the appearance of a minimum or even a discontinuity closer to the front pinhole. Second, a bell-like region of dense plasma is formed at the inner surface of the rear wall (left side on the interferogram). Such a plasma bubble was not observed at the front pinhole on a picosecond time scale. Both effects are induced by presence of the solid walls, where ablative plasma serves as a seeding source of hot electrons, and stimulates higher ionization.

### B. Pinhole size

The parameters of the ablative plasma on the pinholes determine limitations of the pinhole diameter. Indeed, the ionizing beam has to penetrate through the pinholes with minimal interaction, which presupposes larger pinhole diameter. The power density of the laser beam at the pinhole entrance is about $10^{14}$ $W/cm^2$, which is well above the threshold of the ablative plasma formation at the edges of pinholes. Moreover, for wavelength of ~1 $\mu$m, this magnitude is close to the threshold of nonlinear processes in plasma accompanied by generation of plasma waves and fast electrons. The expansion of hot ablative plasma with overcritical density leads to closure of the pinhole aperture due to beam refraction and reflection, similar to the closure effect in spatial filters. The minimization of pressure disturbance inside the gas container, conversely, requires smaller diameters. The optimal size should balance these opposite requirements.

The losses on the pinholes are rather significant and reach ~40–50% at the incident energies of $J_{in}\approx 0.5$ J. These losses are caused by closure of the pinhole aperture due to expansion of overcritical ablative plasma formed at the edges of the pinholes. In order to find optimal pinhole sizes, the shock velocity should be estimated. Such estimation can be done by measuring the energy transmission through the pinhole for different incident beam energies $J_{in}$. The measured values are shown in Fig. 3(a) by dots for two pinhole diameters: 350 and 200 $\mu$m. Assuming Gaussian radial and temporal profiles of the beam, energy transmission can be found by integration over $t$ and $r$, taking the pinhole radius decrease in time with the shock velocity $c_T$,

$$\frac{J_{tr}}{J_{in}}(c_T)=\int_0^{R_0/c_T}\int_0^{R_0-c_Tt}\frac{r}{\tau_b r_b^2\sqrt{2\pi}}\exp\left(-\frac{t^2}{2\tau_b^2}\right)\times\exp\left(-\frac{r^2}{2r_b^2}\right)drdt. \quad (3)$$

The calculated energy transmission is shown in Fig. 3(a) by the solid line, from which the shock velocities were estimated. The dependence of $c_T$ vs $J_{in}$ is shown in Fig. 3(b). The assumed model, however, accounts only for beam reflection, and therefore provides overestimated values of $c_T$, especially for smaller pinhole diameter.

For maximizing the energy transmission, the diameter of the pinholes was close to 350 $\mu$m for the front pinhole and ~150 $\mu$m for the rear one. At smaller diameters of the front pinhole, pinhole losses became too significant, which affects density and uniformity of the plasma channel. Indeed, the beam cross section at the plane of pinholes in vacuum was about $80\times 80$ $\mu$m. The beam was aligned to the center of the pinholes, so the second minimum of intensity profile of the diffraction-limited beam appeared right near the edge of the 350 $\mu$m front pinhole. The energy density in the third maximum, however, is $\sim 1.6\times 10^{-2}$ of the energy density in the central maximum, which is about $10^{12}$ $W/cm^2$. Such energy density is high enough for gradual destruction of the outer surface of the pinhole. Lifetime of the front pinhole was limited by 100–200 pulses at the repetition rate of 1 pulse per minute. Smaller rear pinhole leads to increase of the density and size of the plasma bubble at the rear wall.

At the waist pointing vacuum, the ionizing beam had a diffraction-limited cross section with an approximately 70

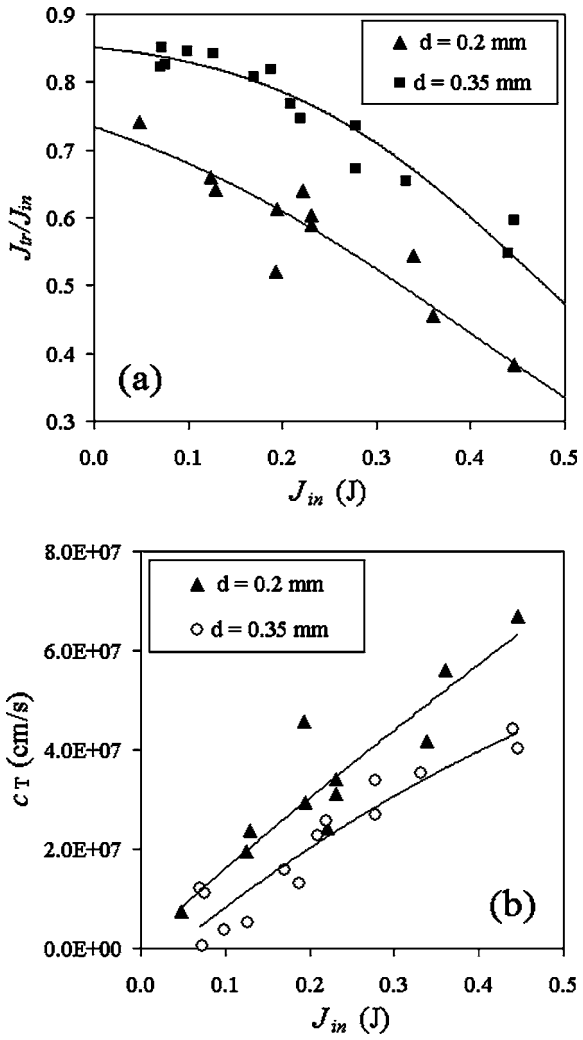


FIG. 3. Energy transmission through pinholes $J_{tr}/J_{in}$ (a), and shock velocity $c_T$ (b), vs incident beam energy $J_{in}$. Front and rear pinhole diameters are 350 and 200 $\mu$m, respectively. Markers in (a) represent measured values, solid lines are calculation via (2).

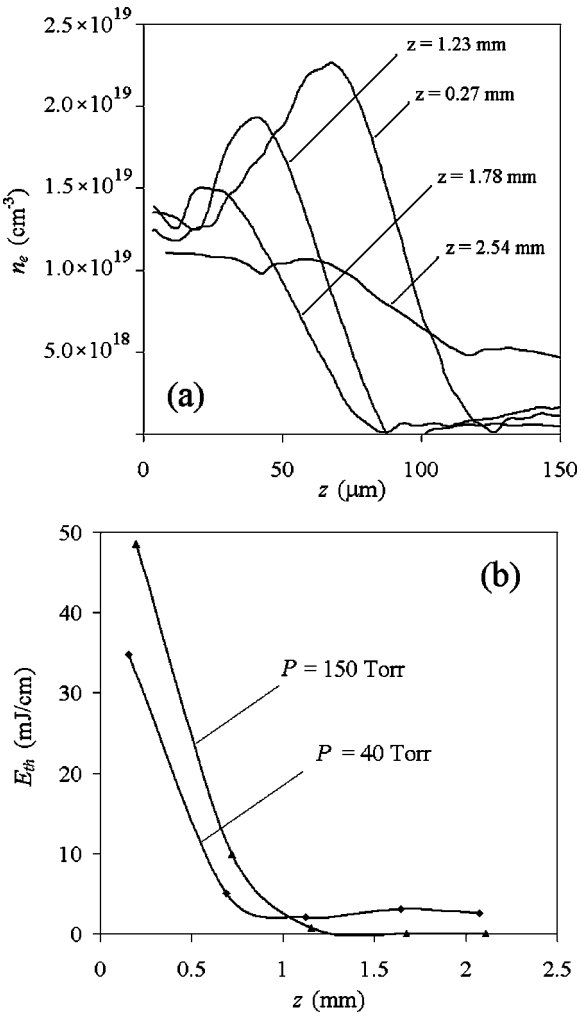


FIG. 4. Radial profiles of the plasma density at $p$=40 Torr $N_2$ (a), and deduced thermal energy $E_{th}$ along the channel (b). $J_{in}$=0.43 J, $t$=800 ps.

$\times 70$ $\mu$m width at the beam waist. The Rayleigh length can be estimated as $Z_R \sim 3.8$ mm, which is about of the length of the gas cylinder. The beam waist was aligned to the middle of the gas cylinder. In this case, vacuum energy density inside the gas cylinder does not change more than twice along the channel, and the plasma channel from the front to the rear pinhole is formed. Displacement of the waist from the middle point leads to significant nonuniformity along the channel. For instance, when the waist was aligned to the plane of the first pinhole, the observable channel did not reach the plasma bubble at the rear pinhole.

### C. Radial profile

The expansion of the plasma channel was found to be similar to the expansion in backfill experiments.[13,14] Indeed, parameters of ionizing beam used in the present set of experiments are close to parameters reported by Clark *et al.*[14] and Durfee *et al.*,[13] and nonflowing gas was ionized. The expansion of the channel in time was studied thoroughly by these authors; thus, we mention here the close similarity of our results to the previously reported temporal behavior. Our interest here is in producing the channel minimal longitudinal changes in the radial profiles of plasma density. A typical example of the radial density profiles at several longitudinal locations in 40 Torr of $N_2$ is shown in Fig. 4(a) for the delay of $\sim$800 ps.

Along the channel, the radial profile changes due to spatially nonuniform energy deposition. Energy deposition in gases at several hundred Torr is usually a few percent of the beam energy. Profile of the energy deposition along the channel depends on the beam convergence, which was confirmed by variation of the position of the beam waist. However, it may be affected by additional stimulating effects, for instance, UV radiation from the dense ablative plasma formed on the walls. Indeed, short channels next to the front pinhole and before the plasma bubble at the rear pinhole were formed at any position of the beam waist, even outside the gas cylinder. Conversely, with oversized pinholes, i.e., in the backfill case, plasma channels with a detectable density did not form at the same pressure and the laser intensity. Thus, we presume that the presence of ablative plasma plays an important role in the channel formation.

The actual profile of the energy deposition may be

roughly estimated from the thermal energy $E_{th}$ of the expanding plasma. Clark *et al.*[14] showed the applicability of the self-similar model of expansion of cylindrical shock wave for estimation of $E_{th}$ from the position of the shock wave front: $R(t)=\xi_0(E_{th}/\rho_0)^{1/4}\tau^{1/2}$. Here $\xi_0 \sim 1$ and $\rho_0$ is the gas density. In spite of uncertainty in absolute values of $E_{th}$ due to strong dependence on $R(t)$, this method can enlighten the longitudinal nonuniformity of the energy deposition.

The longitudinal profiles of $E_{th}$ for different gas pressures are shown in Fig. 4(b). The thermal energy is high near the front pinhole, where the influence of the wall plasma is high. At lower pressures or about 110–120 Torr $N_2$, the energy deposition is uniform between 0.7 and 2.5 mm and stays within 2–5 mJ/cm depending on pressure. This value is close to the thermal energy in the plasma channels measured in the backfill at similar gas pressures.[14] At higher pressures, however, the uniformity disappears, with higher deposition near the entrance of the beam. The increased energy deposition near the front pinhole at higher neutral density might be explained by the increasing influence of the expanding ablative plasma. Hot electrons from the ablative plasma, which penetrates into the neutral gas, might result in the increase of absorption rate at the vicinity of the front pinhole.

Supporting evidence for the hot electron effect comes from attempts to stimulate the dense plasma formation by initiation of an electric discharge in the gas cylinder. While the addition of a low-current glow discharge with the plasma density of about $10^9$ cm$^{-3}$ only slightly improves the uniformity of the channel, a high-current arc discharge leads to formation of a dense, highly nonuniform plasma bubble at the front pinhole, leading to its complete closure.

The radial expansion of the shock wave with formation of the minimum plasma density at the axis was observed in nitrogen, helium, and argon. In xenon, however, the radial profiles of the plasma density differ from those lighter gases (see Fig. 5). Even after about 1 ns from the ionizing laser pulse, the profile maintains a Gaussian-type shape. The density of channels in Xe is about the same as for other gases, but at lower neutral densities. Channels in Xe are usually nonuniform and shorter than the cylinder length. This may be explained by lower ionization potentials and higher mass of Xe atoms, which affects the expansion and ionization, and by influence of the ablative plasma from the front pinhole.

Differences between gases can be illustrated also by the total beam energy transmitted through the gas cylinder, which is a difference between the beam energies measured before and after the gas cylinder. For high-Z gases, energy transmission drops to about 10% at 80–100 Torr and remains at the same level at higher pressures for all gases (see Fig. 6). In helium, however, energy transmission of 31–33% was observed at pressures higher than 300 Torr. The pressure at which the energy transmission reaches its minimal value coincides well with the maximal pressure at which plasma channels with acceptable uniformity may be created. Obviously, the energy transmission is determined mostly by the beam refraction on the ablative plasma near the pinholes, while the actual energy deposition in the gas is below 10%. However, the transmitted energy can be used for monitoring

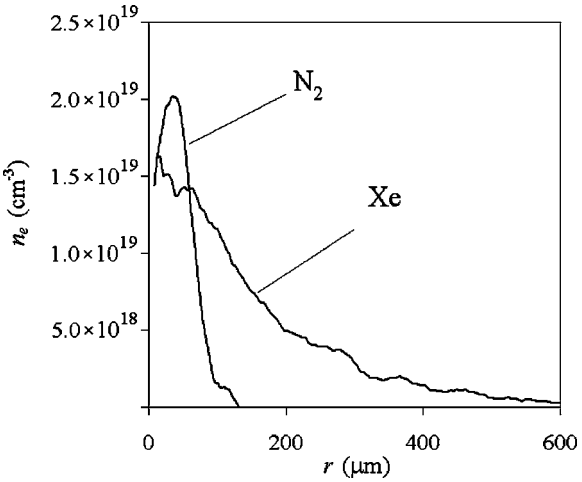


FIG. 5. Radial profiles of the plasma density in $N_2$ and in Xe at $p=60$ Torr. $J_{in}=0.41$ J, $t=800$ ps, $z=0.4$ mm from the front pinhole.

the optimal pressure for the channel formation. At higher pressures, the plasma at the front pinhole becomes denser, which leads to higher beam refraction and correspondingly lower and less uniform energy deposition along the channel.

### D. Longitudinal profile

The uniformity of the plasma channel is optimized at the axis at a certain time from the channel formation. Indeed, the higher the initial density, the higher the expansion rate and the consequent density drop at the axis. Thus, at some point in time, the initially nonuniform channel will have uniform density along its axis. This effect is particularly prominent for nonuniformities induced by the presence of ablative plasma at the entrance and the exit of the gas cylinder. For instance, we found that in nitrogen the axial part of the channel has good uniformity at about 800 ps from the ionizing pulse. The corresponding longitudinal density profiles are presented in Fig. 7. At $P=40$ Torr, the channel had an average density of $7\times10^{18}$ cm$^{-3}$ with nonuniformity of about

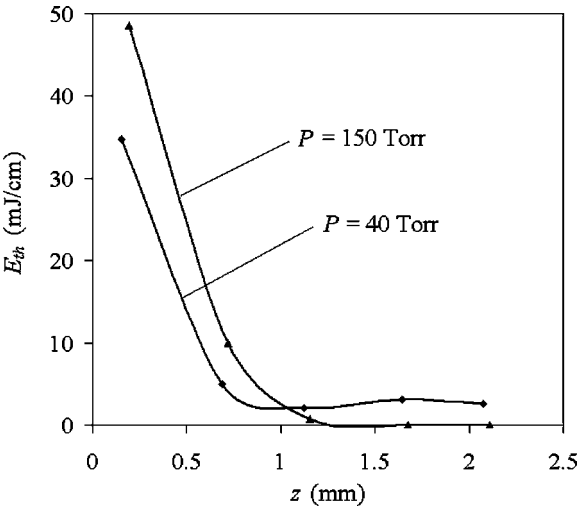


FIG. 6. Total energy transmission through the gas cylinder for different gases.

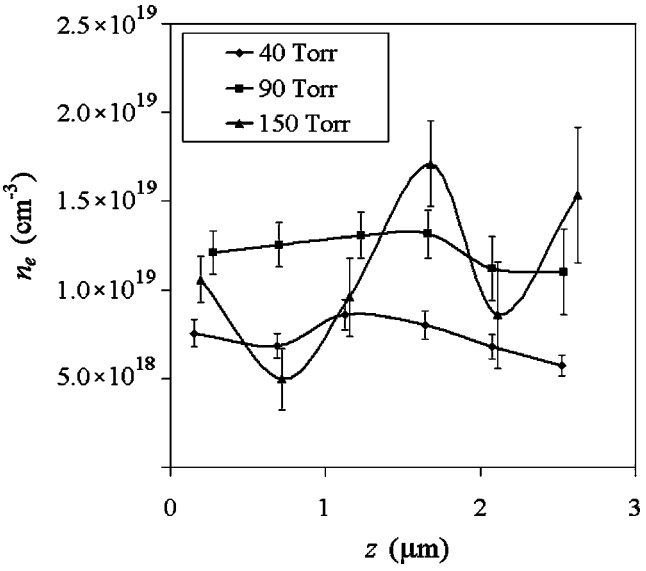


FIG. 7. Longitudinal profiles of the plasma channel in $N_2$. $J_{in}=0.43$ J, $t=800$ ps.

±7.5% on a radius of less than 15 $\mu$m. The best result was observed at $P=40$ Torr, when a channel with nonuniformity of about ±3.5% had a density of $1.2\times10^{19}$ cm$^{-3}$ on a radius of 15 $\mu$m.

The structure of the plasma channel with the average depth of $\delta n_{er}\sim40\%$ [see Fig. 4(a)] might be attractive, for instance, for SRB schemes with strong plasma wave localization.[18,19] It was shown that in the multimode regime, continuum modes of the plasma channel might contract the backscattered beam and increase the growth rate.[20] For our parameters of the channel (density at the axis $n_{e0}\sim1.2\times10^{19}$ cm$^{-3}$ and the average depth of the channel $\Delta n_e\sim40\%$), plasma density gradient exceeds the bandwidth of SRB: $\eta=(\delta n_{er}/n_{e0})/(2\gamma/\omega_{p0})\sim20-50$ for beams with power density of about $10^{14}$ W/cm$^2$. If $\eta>1$, strong plasma wave localization occurs, and SRB amplification would benefit from contraction. Indeed, beams with $\lambda=0.88$ nm and $I\sim5\times10^{14}$ W/cm$^2$ in the plasma channel will fall into appropriate conditions for the continuum mode contribution: $U_1<a_0<U_0$.[20] Here, $U_0=(\delta_r n_e/n_{e0}/2(\omega/\omega_{p0})^{1/2}\sim0.17$, $U_1=U_0/[\pi^{1/2}(2(\omega/\omega p_0)^{3/4})]\sim0.01$, and $a_0=eE/mc\omega\sim0.02$.

## IV. CONCLUSION

The formation of plasma channels in a nonflowing gas, contained in a cylindrical chamber, has been demonstrated. The laser beam passed through the chamber along its axis via pinholes in the chamber walls. The plasma channels, with an electron density on the order of $10^{18}-10^{19}$ cm$^{-3}$, were formed in pure He, $N_2$, Ar, and Xe by a 100 ps Nd:YAG laser beam with energy of about 0.3–0.5 J. Plasma density in the channels reaches the nonuniformity of several percent at a certain time delay, which depends on the gas molecular weight.

In order to achieve the high density necessary for good Raman coupling, high gas pressure is needed, both in flowing jets and in the stationary gas pursued here. Although the pressures that give the most uniform density in the stationary gas are comparable to the pressures achievable in the gas jets, the ultimate technological limitations are likely governed by different physical principles. The effect of ablative plasma formation at the walls is the dominant physical process of plasma creation in the configuration with pinholes. On the other hand, interaction with gas leaking outside the gas cylinder through the pinholes does not impair interaction within the cylinder. Nonetheless, in the window of optimal pressure around 90 Torr for $N_2$, the axial density was comparable to gas jet technology.

In identifying the laser-ablative physics as a key to the overall attainment of plasma uniformity, it appears that further progress in uniformity might entail different techniques: additional surfaces, better control of the geometry and wall materials, or additional sources of preliminary ionization, such as electric discharges or UV radiation. For instance, low-current glow discharge initiated in the chamber improves the uniformity of the plasma channel slightly.

## ACKNOWLEDGMENTS

The authors would like to express their gratitude to Professor S. Suckewer for the use of the Nd:YAG laser of the Department of Mechanics and Aerospace at Princeton University. The gas chamber was built at PPPL with the design assistance of Dr. A. Warshavsky. The assistance of Dr. A. Morozov and N. Tkach is greatly appreciated.

This work was supported in part by the United States Defense Advanced Research Projects Agency (DARPA) and in part by DOE Contract AC02-76CHO-3073, and by the NNSA under SSAA Program through DOE Research Grant DE-FG52-04NA00139.

[1] V. M. Malkin, G. Shvets, and N. J. Fisch, Phys. Plasmas **7**, 2232 (2000); V. M. Malkin, G. Shvets, and N. J. Fisch, Phys. Rev. Lett. **82**, 4448 (1999).
[2] G. Shvets, N. J. Fisch, A. Pukhov, and J. Meyer-ter-Vehn, Phys. Rev. Lett. **81**, 4879 (1998); G. Shvets, N. J. Fisch, A. Pukhov, and J. Meyer-ter-Vehn, Phys. Plasmas **10**, 2056 (2004).
[3] V. M. Malkin and N. J. Fisch, Phys. Plasmas **8**, 4698 (2001); D. S. Clark and N. J. Fisch, Phys. Plasmas **10**, 3363 (2003).
[4] N. J. Fisch and V. M. Malkin, Phys. Plasmas **10**, 2056 (2003).
[5] W. Cheng Y. Avitzour, Y. Ping, S. Suckewer, N. J. Fisch, M. S. Hur, J. S. Wurtele, Phys. Rev. Lett. **94**, 045003 (2005).
[6] A. A. Solodov, V. M. Malkin, and N. J. Fisch, Phys. Plasmas **10**, 2540 (2003).
[7] Y. Ping, I. Geltner, N. J. Fisch, G. Shvets, and S. Suckewer, Phys. Rev. E **62**, R4532 (2000).
[8] Y. Ping, I. Geltner, A. Morozov, N. J. Fisch, and S. Suckewer, Phys. Rev. E **66**, 046401 (2002).
[9] A. Balakin,, D. V. Kartashov, A. M. Kiselev, S. A. Skobelev, A. N. Stepanov, and G. M. Fraiman, JETP Lett. **80**, 12 (2004).
[10] Y. Ping, W. Cheng, S. Suckewer, D. S. Clark, and N. J. Fisch, Phys. Rev. Lett. **92**, 175007 (2004).
[11] C. G. Durfee III and H. M. Milchberg, Phys. Rev. Lett. **71**, 2409 (1993).
[12] H. M. Milchberg, T. R. Clark, C. G. Durfee III, and T. M. Antonsen, Phys. Plasmas **3**, 2149 (1996).
[13] C. G. Durfee III, J. Lynch, and H. M. Milchberg, Phys. Rev. E **51**, 2368 (1995).
[14] T. R. Clark and H. M. Milchberg, Phys. Plasmas **7**, 2192 (2000).
[15] E. W. Gaul, S. P. Le Blanc, A. R. Rundquist, R. Zgadzaj, H. Langhoff, and M. C. Downer, Appl. Phys. Lett. **77**, 4112 (2000).

[16]G. Pretzler, Z. Naturforsch., A: Phys. Sci. **46a**, 639 (1991).
[17]S. August, D. Strickland, D. D. Meyerhofer, S. L. Chin, and J. H. Eberly, Phys. Rev. Lett. **63**, 2212 (1989).
[18]P. Mardahl, H. J. Lee, G. Penn, J. S. Wurtele, and N. J. Fisch, Phys. Lett. A **296**, 109 (2002).
[19]I. Y. Dodin, G. M. Fraiman, V. M. Malkin, and N. J. Fisch, JETP **95**, 625 (2002).
[20]S. Yu. Kalmykov and G. Shvets, Phys. Plasmas **11**, 4686 (2004).